

## Microwave-Assisted Self-Organization of Colloidal Particles in Confining Aqueous Droplets

Shin-Hyun Kim,<sup>†</sup> Su Yeon Lee,<sup>†</sup> Gi-Ra Yi,<sup>‡,⊥</sup> David J. Pine,<sup>§</sup> and Seung-Man Yang<sup>\*,†</sup>

*Contribution from the National Creative Research Initiative Center for Integrated Optofluidic Systems and Department of Chemical and Biomolecular Engineering, Korea Advanced Institute of Science and Technology, Daejeon, 305-701, Korea, Corporate R&D Center, LG Chem Research Park, Daejeon, 305-380, Korea, and Department of Physics, New York University, New York, New York 10003*

Received May 20, 2006; E-mail: smyang@kaist.ac.kr; yigira@kbsi.re.kr

**Abstract:** Monodisperse aqueous emulsion droplets encapsulating colloidal particles were produced in the oil phase, and controlled microwave irradiation of the aqueous drop phase created spherical colloidal crystals by so-called evaporation-induced self-organization of the colloidal particles. Unlike usual colloidal crystals, colloidal crystals in spherical symmetry (or photonic balls) possessed photonic band gaps for the normal incident light independent of the position all over the spherical surface. While the consolidation of colloidal particles in emulsion droplets in an oven took several hours, the present microwave-assisted evaporation could reduce the time for complete evaporation to a few tens of minutes. Under the microwave irradiation, the aqueous phase in emulsions was superheated selectively and the evaporation rate of water could be controlled easily by adjusting the microwave intensity. The result showed that the packing quality of colloidal crystals obtained by the microwave-assisted self-organization was good enough to show photonic band gap characteristics. The reflectance of our photonic balls responded precisely to any change in physical properties including the size of colloidal particles, refractive index mismatch, and angle of the incident beam. In particular, for polymeric particles, the photonic band gap could be tuned by the intensity of microwave irradiation, and the reflection color was red-shifted with stronger microwave irradiation. Finally, for better photonic band gap properties, inverted photonic balls were prepared by using the spherical colloidal crystals as sacrificial templates.

### Introduction

Self-assembly, in which building blocks are organized spontaneously into bulk thermodynamic phases, has attracted great attention in materials chemistry and soft condensed-matter physics. However, most of self-assembled structures have always contained undesired defects, and the ordered arrangement and the packing structure cannot be controlled with ease. Over the years, for prescribing lattice positions of the building blocks or bulk shapes, confined geometries have been introduced to self-organization by several research groups. For instance, the confined geometry effect of microchannels<sup>1</sup> or capillary tubes<sup>2,3</sup> produced relatively well ordered structures of colloids, and an array of square pyramidal pits created colloidal crystals with facing (100) planes,<sup>4</sup> which could not be formed otherwise. Recently, we developed the emulsion-based route to creating spherical shaped colloidal crystals all of equal size or colloidal

polyhedra of unique configurations. In this case, emulsion droplets provided the geometrical confinement for the self-assembly of colloidal particles. Specifically, colloidal particles in confining droplets were self-organized into colloidal clusters as the droplets were shrunk by slow evaporation of the liquid phase of the droplets in an oven. When the number of colloidal particles in a droplet was large, they formed a spherical colloidal crystal<sup>5–9</sup> (or photonic ball) which exhibited an optical stop band for the normal incident light independent of the position all over the spherical surface. Meanwhile, for a small number (<15) of colloidal particles, they were consolidated into colloidal polyhedra<sup>10,11</sup> of which the configuration and optical scattering spectrum were unique depending only on the number of the constituting particles.

In this article, we demonstrate that monodisperse colloidal particles inside emulsion droplets can be organized into colloidal

<sup>†</sup> Korea Advanced Institute of Science and Technology.

<sup>‡</sup> LG Chem Research Park.

<sup>§</sup> New York University.

<sup>⊥</sup> Present address: Nano-Bio System Research Team, Seoul Center, Korea Basic Science Institute, Seoul 136-713 Korea.

(1) Kim, E.; Xia, Y.; Whitesides, G. M. *Adv. Mater.* **1996**, *8*, 245–247.

(2) Moon, J. H.; Kim, S.; Yi, G.-R.; Lee, Y.-H.; Yang, S.-M. *Langmuir* **2004**, *20*, 2033–2035

(3) Kamp, U.; Kitaev, V.; Freymann, G. von; Ozin, G. A.; Mabury, S. A. *Adv. Mater.* **2005**, *17*, 438–443

(4) Yin, Y.; Xia, Y. *Adv. Mater.* **2002**, *14*, 605–608

(5) Yi, G.-R.; Manoharan, V. N.; Klein, S.; Brzezinska, K. R.; Pine, D. J.; Lange, F. F.; Yang, S.-M. *Adv. Mater.* **2002**, *14*, 1137–1140

(6) Moon, J. H.; Yi, G.-R.; Yang, S.-M.; Pine, D. J.; Park, S. B. *Adv. Mater.* **2004**, *16*, 605–609

(7) Iskandar F.; Chang, H.; Okuyama, K. *Adv. Powder Technol.* **2003**, *14*, 349–367

(8) Iskandar, F.; Mikrajuddin; Okuyama, K. *Nanoletters* **2001**, *1*, 231–234

(9) Velev, O. D.; Lenhoff, A. M.; Kaler E. W. *Science* **2000**, *287*, 2240–2243

(10) Manoharan, V. N.; Elsesser, M. T.; Pine, D. J. *Science* **2003**, *301*, 483–487

(11) Yi, G.-R.; Manoharan, V. N.; Michel, E.; Elsesser, M. T.; Yang, S.-M.; Pine, D. J. *Adv. Mater.* **2004**, *16*, 1204–1208

crystals by microwave irradiation. Microwaves have been used traditionally for demulsification by selective heating<sup>12–14</sup> and recently for synthesis and assembly of nanoparticles<sup>15–17</sup> and polymeric latexes<sup>18–20</sup> by its special features. Microwaves can selectively superheat polar molecules through dipole rotation and ionic conduction without affecting nonpolar molecules such as hydrocarbon oils. Once microwaves are irradiated into a water-in-oil emulsion, the water molecules in the emulsion are heated selectively, evaporated to diffuse into the oil phase, and eventually transported into ambient air. Compared with conventional heat-up, microwave heating can reduce considerably the time required for a complete consolidation of colloidal particles keeping the emulsion stable. Our precedent results showed that thermodynamic equilibrium driven diffusion of water from the emulsion droplets to the continuous phase of silicone oil took approximately 12 h at room temperature for a complete consolidation, and heating at 70 °C reduced the required time to several hours. However, microwave irradiation enabled us not only to control readily the evaporation rate of water but also to create the spherical colloidal crystals in very short times usually within 10 min. Furthermore, the present method of microwave-assisted fabrication is particularly useful for tuning photonic band gaps of colloidal crystals of polymeric latex particles, which is practically important but not easy to achieve. The polymeric latexes are annealed and experience viscoelastic deformation above glass transition temperature at a sufficiently strong irradiation intensity. Therefore, the packing density of polymeric latex particles will be increased at higher intensities, which in turn tune the photonic band gaps toward longer wavelengths.

In the subsequent sections, we will begin with the fabrication of uniform photonic balls of silica or polymeric microspheres and inverse opaline photonic balls from uniform emulsion droplets generated by a so-called shear rupturing mode of drop breakup.<sup>21</sup> Then, we will discuss how the microwave intensity affects the evaporation rate and the packing quality of the colloidal particles in photonic balls made from water-in-oil emulsions. Finally, we will examine the optical properties associated with highly ordered packings of the colloidal particles and their inverse structures.<sup>22</sup>

### Preparation of Monodisperse Emulsion Droplets and Microwave-Assisted Crystallization

Equal-sized emulsion droplets at micrometer scales could be produced by continuous drop breakup in microfluidic devices with T-junction channels<sup>23</sup> or capillary tubes with micron-sized holes. Recently, more complex geometries of channels or microtubes have been developed for additional flexibility in

controlling the droplet size or shape. In this study, we used a droplet break-off technique in a coflowing stream,<sup>21</sup> in which the diameter of emulsion droplets could be easily controlled by the inner diameter of a micropipet and the velocity of the coflowing stream. Monodisperse aqueous emulsion droplets were prepared by injecting an aqueous colloidal suspension of silica or PS microspheres into a micropipet, with the tip of the micropipet dipped into hexadecane in the rotating Teflon bath. For a stable water-in-oil emulsion, 1% wt/wt nonionic surfactant (Hypermer 2296) was added to the hexadecane phase. Pressurized nitrogen gas pushed the suspension in the micropipet into the hexadecane phase. The protruded suspension was then broken into emulsion droplets under the action of viscous force exerted by the rotating hexadecane. For inverse photonic balls, a binary suspension of silica nanoparticles and PS microspheres was injected into a micropipet. Detailed experimental procedures and materials were described in the Supporting Information. Although the size of the emulsion droplets deviated slightly depending on the contents of the emulsion phase, the emulsion droplets of 75  $\mu\text{m}$  and 140  $\mu\text{m}$  in average diameter were produced from the micropipets with 10  $\mu\text{m}$  and 30  $\mu\text{m}$  tips, respectively. Figure 1a and 1b show the optical micrographs of highly monodisperse emulsion droplets dispersed in hexadecane. Indeed, the present emulsification method via the shear rupturing mode of drop breakup did not produce any satellite droplets, and the size of emulsion droplets was quite uniform. The silica microspheres encapsulated in each emulsion droplet were not recognizable in optical micrographs since their size was 240 nm.

The colloidal particles were consolidated into spherical opaline structure as the water in the emulsion droplets was removed by microwave irradiation, as schematically illustrated in Figure 1c. The consolidation time was dependent on the microwave intensity and was identified by an appearance of iridescent opaline color, which was a clear evidence for the formation of spherical colloidal crystals or photonic balls. The emulsion droplets of 75  $\mu\text{m}$  in diameter were treated at four different microwave intensities, 170, 333.2, 561, and 788.8 W.

In Figure 2, the diameter of emulsion droplets which contained 240 nm silica microspheres was plotted versus the irradiation time in each mode. As noted, the size of emulsion droplets was reduced during superheating, and the time required for a complete consolidation became shorter with higher intensity of irradiation. The SEM images of spherical colloidal crystals of 240 nm silica microspheres, which were consolidated by microwave irradiation in 170 W, were shown in Figure 3a–c. The resulting spherical colloidal crystals were 18  $\mu\text{m}$  in diameter. The size of spherical assemblies was consistent with the prediction from a simple calculation assuming that silica microspheres were packed into face centered cubic (fcc) symmetry. The SEM image in Figure 3a shows the surface morphology of photonic balls exhibiting hexagonally packed microspheres. In particular, the SEM image in Figure 3c shows moiré fringes that are evidence of well-ordered surface packing. This moiré fringes were caused by interaction between a scanning line pattern of an electron microscope and hexagonal lattices of colloidal spheres at a specific magnification as shown in Figure 3d. Here, A is a planar hexagonal colloidal lattice, and B is a scanning line pattern. As noted, a linear moiré pattern was formed for a planar colloidal crystal,<sup>24</sup> and the interval

- (12) Xia, L.-X.; Lu, S.-W.; Cao, G.-Y. *Chem. Eng. Commun.* **2004**, *191*, 1053–1063.
- (13) Chan, C.-C.; Chen, Y.-C. *Sep. Sci. Technol.* **2002**, *37*, 3407–3420.
- (14) Fang, C. S.; Chang, B. K. L.; Lai, P. M. C. *Chem. Eng. Commun.* **1988**, *73*, 227–239.
- (15) Gerbec, J. A.; Magana, D.; Washington, A.; Strouse, G. F. *J. Am. Chem. Soc.* **2005**, *127*, 15791–15800.
- (16) Gao, F.; Lu, Q.; Komarneni, S. *Chem. Mater.* **2005**, *17*, 856–860.
- (17) Yu, J. C.; Hu, X.; Li, Q.; Zhang, L. *Chem. Commun.* **2005**, 2704–2706.
- (18) Correa, R.; Gonzalez, G.; Dougar, V. *Polymer* **1998**, *39*, 1471–1474.
- (19) Bao, J.; Zhang, A. *J. Appl. Polym. Sci.* **2004**, *93*, 2815–2820.
- (20) He, W.-D.; Pan, C.-Y.; Lu, T. *J. Appl. Polym. Sci.* **2001**, *80*, 2455–2459.
- (21) Umbanhowar, P. B.; Prasad, V.; Weitz, D. A. *Langmuir* **2000**, *16*, 347–351.
- (22) Schroden, R. C.; Al-Daous, M.; Blandford C. F.; Stein, A. *Chem. Mater.* **2002**, *14*, 3305–3315.
- (23) Thorsen, T.; Roberts, R. W.; Arnold F. H.; Quake, S. R. *Phys. Rev. Lett.* **2001**, *86*, 4163–4166.

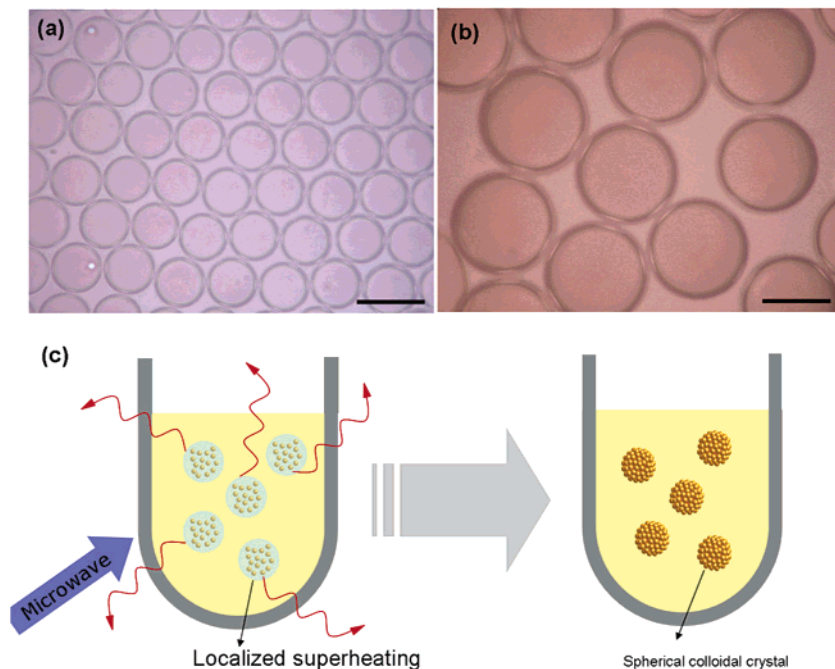


**Figure 1.** Optical microscope images of the monodisperse emulsions of (a) 75  $\mu\text{m}$  in average diameter by using a micropipet of 10  $\mu\text{m}$  in inner diameter and (b) 140  $\mu\text{m}$  in average diameter by using a micropipet of 30  $\mu\text{m}$  in inner diameter. The emulsion droplets contained silica particles of 240 nm in diameter. (The scale bar is 100  $\mu\text{m}$ .) (c) Schematic of microwave-assisted fabrication of photonic balls. The microwave excites the water molecules and superheats the emulsion phase. After evaporation of water, the spherical colloidal crystals are formed through self-assembly of colloidal particles.

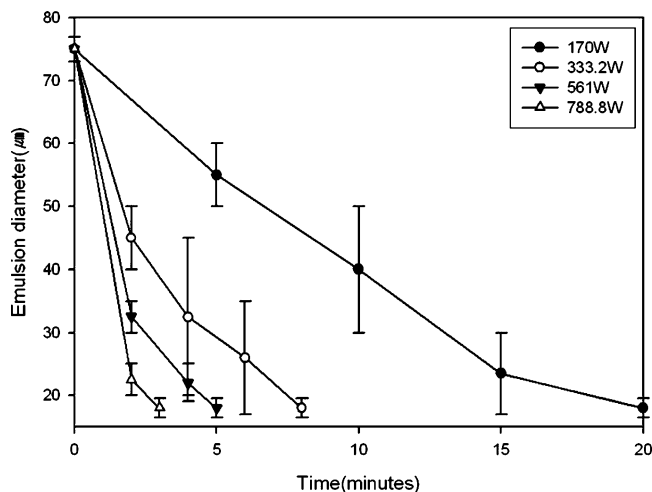


**Figure 2.** Size change of the emulsion droplets with the irradiation time for 170, 333.2, 561, and 788.8 W. Monodisperse silica spheres of 240 nm in diameter were dispersed inside of the aqueous emulsion droplets.

between neighboring moiré fringes was changed by the orientation of the scanning line pattern relative to the hexagonal lattices. In case of spherical colloidal crystals, the moiré fringe exhibited a nonlinear pattern because the lattice constant along the projection direction changed due to the spherical surface curvature. The images in Figure 3e and 3f were obtained in different magnifications by overlapping the line pattern (as a model of scanning lines of electron microscope) onto the SEM images of the spherical colloidal crystal in Figure 3b. Indeed, the overlapped images produced an interaction pattern similar to the moiré pattern of Figure 3c, which clearly confirmed the well-ordered surface packing, as well as the spherical surface curvature of colloidal crystals.

### Optical Properties of Silica Photonic Crystal Balls

As we described previously, the reflection spectra of a photonic ball were not changed by the rotation of the ball for a fixed incident angle of light.<sup>6</sup> This was because the surface of a spherical ball was the (111) plane of fcc packing symmetry, which was induced by the surface confinement effect of the spherical emulsion drop during colloidal crystallization. However, as shown in Figure 4, reflected colors of the photonic balls composed of 257 nm silica particles in hexadecane were modulated as the angle between the incident light and the direction of view were changed. As the angle was decreased from 90° to 10°, the reflection spectra were shifted from blue to red. The photonic balls behave like an optical prism because the reflected color of white light depended on the viewing angle.

The wavelengths  $\lambda$  of reflected light can be estimated by Bragg's law for a composite colloidal crystal which is composed of two dielectric materials with refractive indices  $n_i$  ( $i = 1, 2$ ) and volume fraction  $V_i$ :

$$\lambda = 2dn_{\text{eff}} = \left(\frac{8}{3}\right)^{1/2} D \left( \sum_i n_i^2 V_i - \sin^2 \phi \right)^{1/2}$$

in which  $d$  is the characteristic spacing,  $D$ , the particle size and  $\phi$ , the angle between the incident beam and the (111) direction of fcc stacking. It can be expected from Bragg's law that the reflection spectra of photonic balls are also modulated by the refractive index mismatch between the microspheres and the medium. To measure the reflection spectra, the silica photonic balls with refractive index  $n = 1.45$  were dispersed in various media including air, water, and hexadecane with different refractive indices  $n = 1.0, 1.33, \text{ and } 1.43$ , respectively. The reflectance spectra in Figure 5a show that the reflectance peak of the silica photonic balls was shifted to higher wavelengths as the refractive index of the dispersed medium was increased.

(24) Subramania, G.; Constant, K.; Biswas, R.; Sigalas, M. M.; Ho, K.-M. *Adv. Mater.* **2001**, *13*, 443–446.

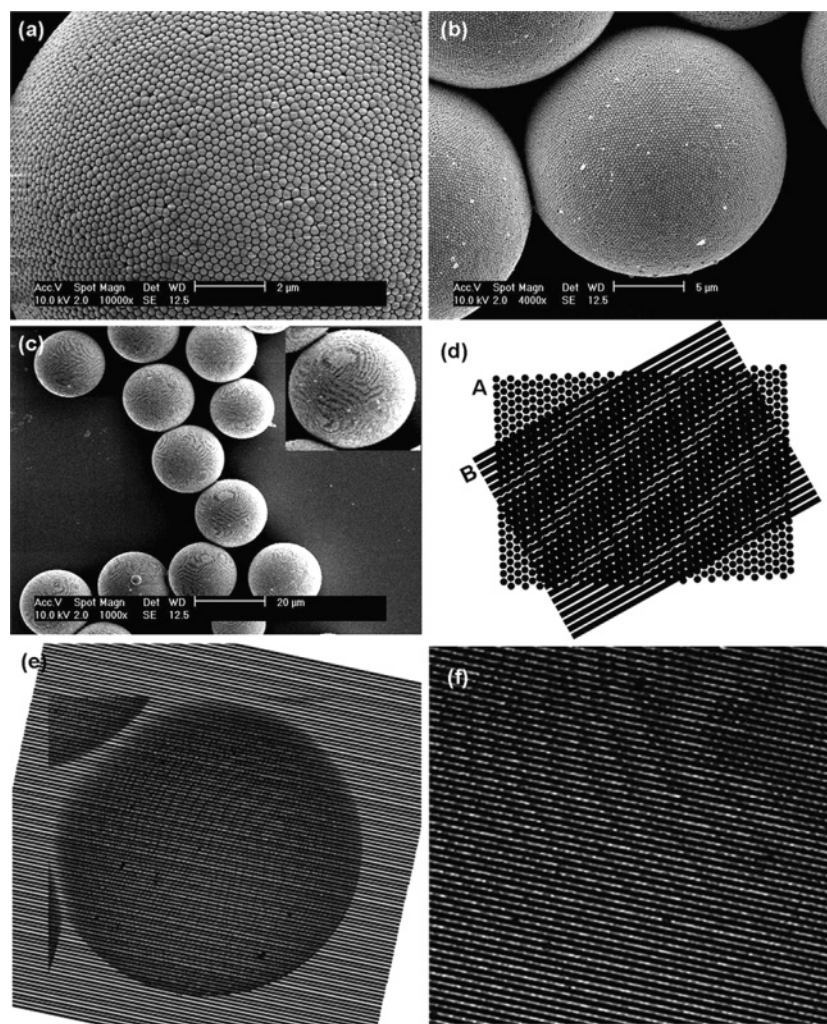


**Figure 3.** SEM images of the spherical colloidal crystals composed of monodisperse silica spheres of 240 nm in diameter at various magnifications. The scale bars in (a), (b), and (c) are 2  $\mu\text{m}$ , 5  $\mu\text{m}$ , and 20  $\mu\text{m}$ , respectively. (d) Overlapped image of the planar hexagonal spot and the line pattern. (e) Overlapped image of the spherical colloidal crystal in (b) and the line pattern. (f) Magnified image of (e).

It is obvious that small deviations in the positions of microspheres from the crystal lattices cause strong scattering, which is especially true when the photonic balls are dispersed in a high refractive index contrast medium. Indeed, as shown in Figure 5a, the reflectance peak broadened as the refractive index contrast was increased. To obtain better reflectance spectra minimizing the undesired scattering, the silica photonic balls were immersed in a prepolymer solution of polydimethylsiloxane (PDMS) which was then cured after the prepolymer solution infiltrated into the interstices between the silica microspheres. Figure 5b shows the optical image of two photonic balls which were prepared with 230 and 257 nm silica microspheres and embedded in a PDMS matrix with refractive index  $n = 1.45$ . Indeed, as shown in Figure 5b and 5c, the photonic balls embedded in the PDMS rubber, which allowed a reducing refractive index mismatch, produced much clearer reflecting colors and reflectance spectra. According to Bragg's law, the reflectance spectra were affected also by the change in the size of the constituting microspheres. As noted from Figure 5c, the maximum reflection peak in the PDMS medium was blue-shifted as the size of the constituent microspheres in each photonic ball was decreased.

According to our observation, the overall size of photonic balls did not affect the reflection color as long as its size was

larger than a critical size of a few tens of micrometers, which was required for the formation of a colloidal crystal shell that was composed of a few well-packed stacking layers of the microspheres. It can be readily expected that the microsphere packing around the central core of a photonic ball is coarse relative to the packing around the outer shell side. This nonuniform packing was induced by the evaporation induced migration of colloidal particles inside of the emulsion droplets. The number of well-packed layers was related with evaporation rate and colloid mobility, and the packing quality affected the intensity of the reflection spectra. The effect of microwave intensity on the packing quality was examined using emulsion droplets of 140  $\mu\text{m}$  and the silica particles of 260 nm in diameter. Figure 6 shows the overall and local surface SEM images of the photonic balls fabricated in five different microwave intensities, 0 (without microwave irradiation), 170, 333.2, 561, and 788.8 W. As noted, however, these SEM images cannot elucidate the packing quality of the microwave-assisted photonic balls because they show only the hexagonal arrangements of microspheres on the surface of photonic balls. To see the internal packing quality indirectly, the reflectance spectra were measured as a function of the microwave intensity, and the result was reproduced in Figure 7. As expected, the reflectance spectra of the photonic balls self-assembled at the

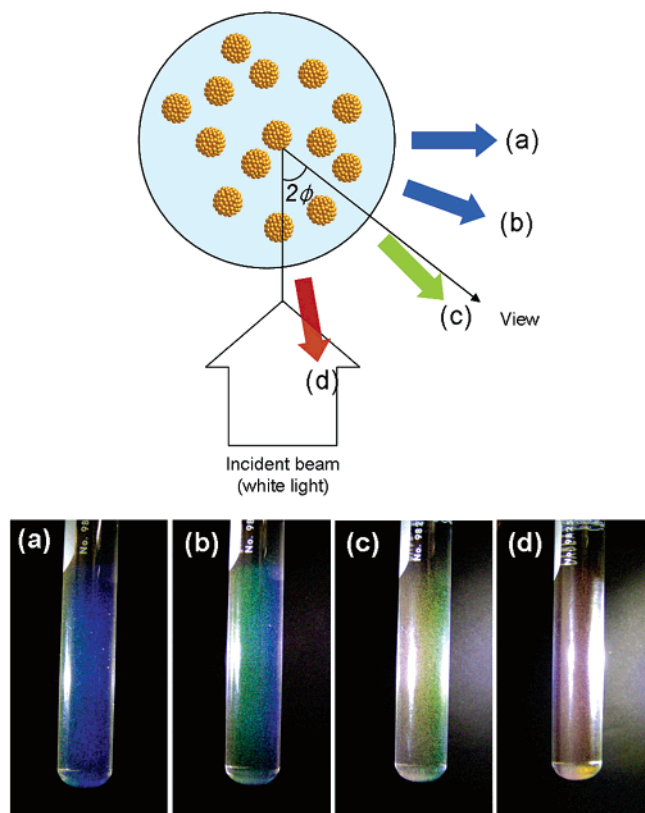


**Figure 4.** Reflective colors of supraballs in hexadecane with a schematic illustration. At (a) 90°, (b) 70°, (c) 45°, and (d) 10° between the incident beam and the viewing direction. The supraballs were composed of silica spheres of 257 nm in diameter and dispersed in hexadecane.

slowest evaporation rate (0 W) had the sharpest peak. Although the peak intensity attenuated as the microwave intensity increased, the reflective color was still as clear as that from the case of 0 W. Therefore, the microwave-assisted photonic balls can be used as color pigments, scatterers, and diffusers. It is also noteworthy that the reflection peaks of the silica colloidal crystals did not shift by the irradiation intensity, which was quite different from the polymeric colloidal crystals as we shall see shortly.

To examine the optical properties as a function of the packing quality, the internal packing structure was observed directly by a confocal laser scanning microscope. A detailed procedure for the confocal microscopy and the resulting confocal microscope images were contained in the Supporting Information. As noted from the confocal microscope images in Figure S1 of the Supporting Information, photonic balls fabricated at 0 W showed well-packed concentric layers. Also, photonic balls prepared at 170 W had a good packing quality, which was comparable with those at 0 W. However, as the microwave intensity was increased further, the packing quality became poor as shown in the confocal microscope image of Figure S1 for a photonic ball produced at 788.8 W. In this strong microwave irradiation, the silica microspheres were packed into a hexagonal arrangement only on the surface of the ball. The overall feature of the internal packing structures at different irradiation intensities was consistent with the optical properties of the photonic balls.

#### Optical Properties of PS Photonic Crystal Balls

Monodisperse PS microspheres of 267 nm in diameter were also used instead of silica microspheres. For proper dispersion

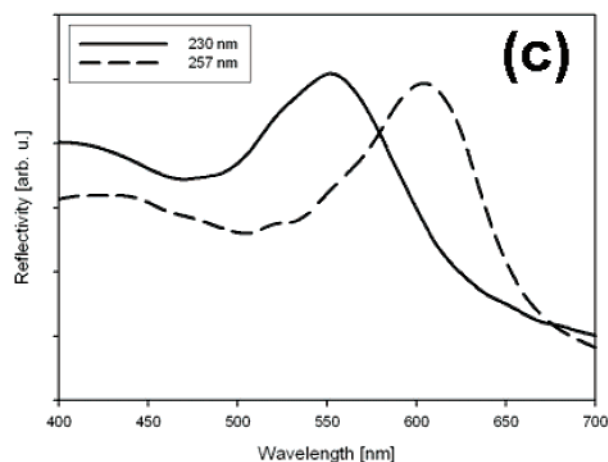
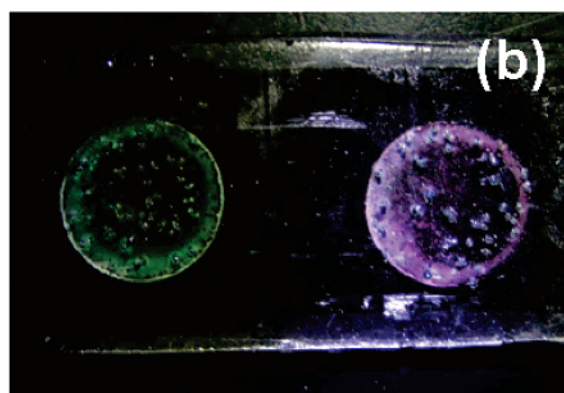
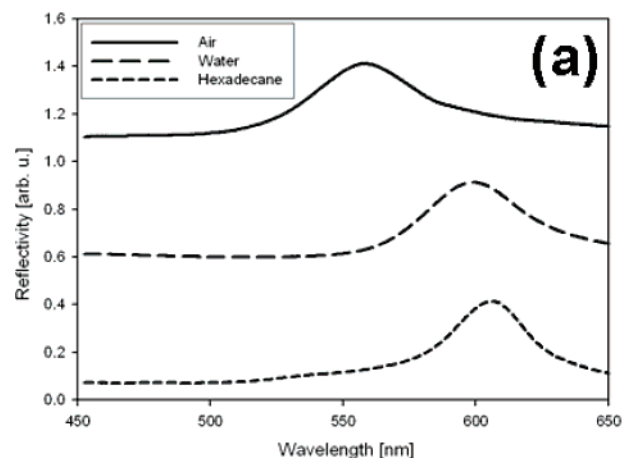


**Figure 5.** (a) Reflectance spectra of the spherical colloidal crystals. The supraballs were dispersed in air, water, and hexadecane and composed of monodisperse silica spheres of 257 nm in diameter. As the refractive index of the medium increased, the reflectance peak shifted to higher wavelengths. (b) Optical image of the supraballs embedded in PDMS. The supraballs were composed of monodisperse silica microspheres of 230 or 257 nm in diameter and (c) their reflectance spectra in PDMS.

stability, PS spheres were synthesized with potassium persulfate as an initiator so that the particle surface was functionalized with sulfate groups. By using the glass micropipet of 30  $\mu\text{m}$  in inner diameter, we produced emulsion droplets of 140  $\mu\text{m}$  in diameter containing 5% wt/wt PS microspheres. Then, the emulsion droplets were irradiated at different intensities. The SEM images of the prepared PS photonic balls are shown in Figure 8. Also included in the insets for comparison are the magnified surface SEM images showing the surface arrange-

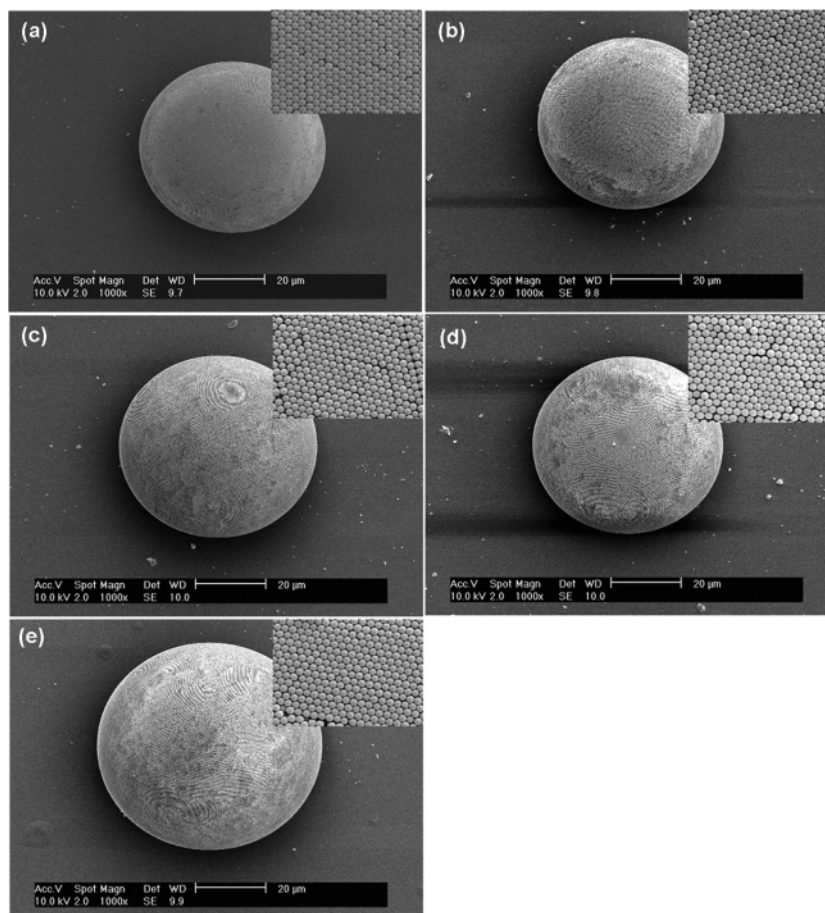


**Figure 6.** SEM images of the spherical colloidal crystals composed of 260 nm silica particles fabricated in different microwave intensities: (a) in 0 W, for 2 days; (b) in 170 W, for 20 min; (c) in 333.2 W, for 8 min; (d) in 561 W, for 5 min; (e) in 788.8 W, for 3 min.

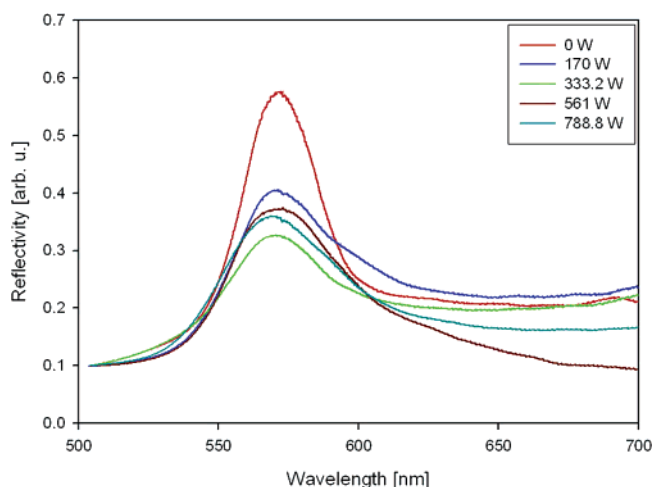


**Figure 7.** Reflectance spectra of the spherical colloidal crystals composed of 260 nm silica particles for various microwave intensities; namely, 0, 170, 333.2, 561, and 788.8 W.

ments of the PS microspheres. Without (0 W) or with a weak irradiation (170 W), the PS spheres were point-contacted on the surface of the photonic balls and arranged into a hexagonally close-packed structure, as shown in Figure 8a and 8b. However, as the microwave intensity exceeded a certain critical value, the emulsion temperature rose above  $T_g$  (glass transition temperature, 100 °C) of polystyrene. Therefore, at a stronger irradiation, the PS particles experienced viscoelastic deformation

and eventually lost the spherical shape.<sup>25</sup> Indeed, as shown in Figure 8c, the PS particles of a photonic ball fabricated at 333.2 W were nonspherical and packed into a face-contacted hexagonal array on the surface. At even higher intensities, small PS particles were coalesced forming one big sphere as noted from Figure 8d for 561 W. At high intensities, the viscoelastic PS particles began to contact each other, and the compressive capillary force pushed them tightly after contact as the water continued to evaporate. The compressive capillary force was responsible for the face-contacted close-packed structure or coalescence at high irradiation intensities.

Because the annealed structure was more closely packed and had a larger density than the nonannealed one, the stop band gap could be tuned by the irradiation intensity.<sup>26</sup> Reflectance data were plotted in Figure 9 for nonannealed and annealed structures. The reflectance peak which appeared in 636 nm for the nonannealed particle assemblies was shifted to 676 nm. This red-shift was caused by the annealing-induced shrinkage of the interstitial space from 26% (for fcc stacking of spheres) to below 8%, which was calculated by Bragg's law with a constant interparticle distance.

The PS photonic balls also showed reflectance colors which changed with the angle between the incident light and the direction of view. When the angle was changed from 90° to 10°, the reflection spectra in hexadecane were shifted from blue to the infrared range as shown in Figure 10.

(25) Mazur, S.; Beckerbauer, R.; Buckholz, J. *Langmuir* **1997**, *13*, 4287–4294.

(26) Gates, B.; Park, S. H.; Xia, Y. *Adv. Mater.* **2000**, *12*, 653–656.

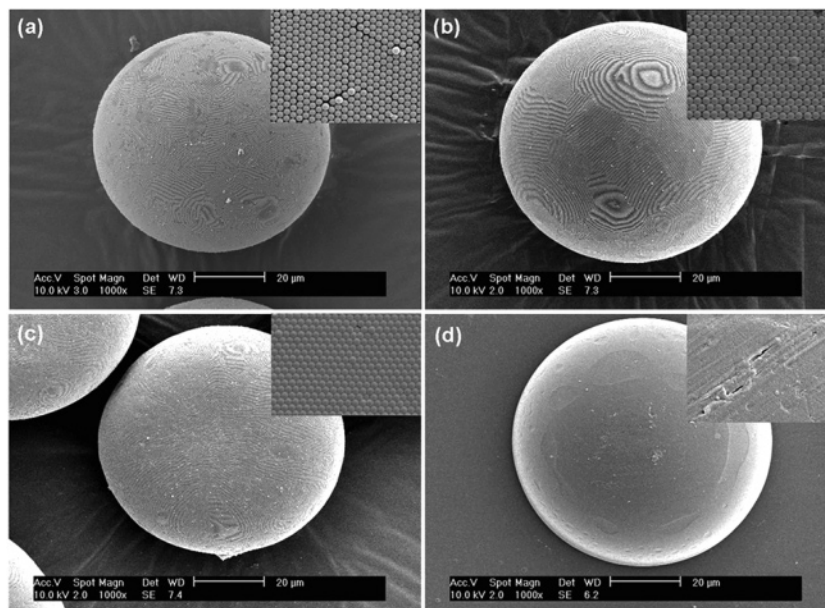


**Figure 8.** SEM images of the spherical colloidal crystals composed of 267 nm PS particles fabricated in different microwave intensities: (a) in 0 W, for 2 days; (b) in 170 W, for 20 min; (c) in 333.2 W, for 8 min; and (d) in 561 W, for 5 min.

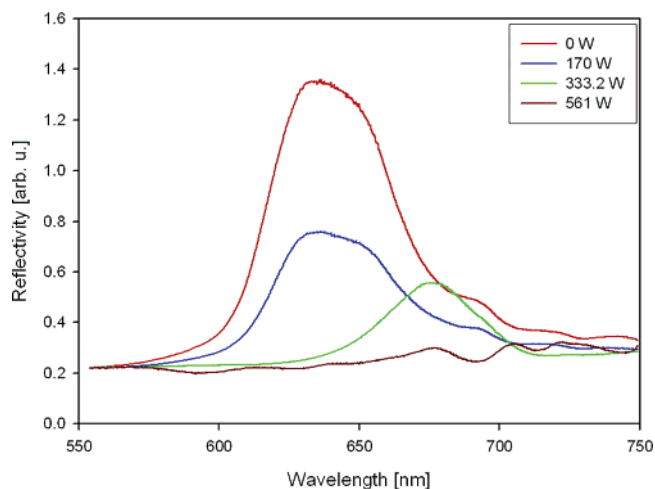


**Figure 9.** Reflectance spectra of the spherical colloidal crystals composed of 267 nm PS particles for various microwave intensities, namely, 0, 170, 333.2, and 561 W.

### Optical Properties of Inverse Silica Photonic Crystal Balls

For inverse structures, we used a binary mixture of PS microspheres of 267 nm in diameter and 30 nm silica nanoparticles. A 1% wt/wt PS suspension and 1% wt/wt silica nanoparticle suspension were mixed with a volume ratio of 2:1, and the mixture suspension was injected in a micropipet of 30  $\mu\text{m}$  in inner diameter. The emulsions were treated at 170 W for 20 min, and the binary colloidal particles were consolidated inside of the emulsion droplets. In the composite colloidal crystals, the silica nanoparticles were filled at the interstices between the PS microspheres. Then, the composite photonic balls were heated to 300  $^{\circ}\text{C}$  for 5 h to remove the PS particles with the silica nanoparticles forming the matrix of the inverse photonic ball as shown in Figure 11. The resulting inverse opaline photonic balls remained spherical with hexagonally ordered spherical cavities. The reflectance data in Figure 12 show that the band gap of the inverse opaline balls was blue-

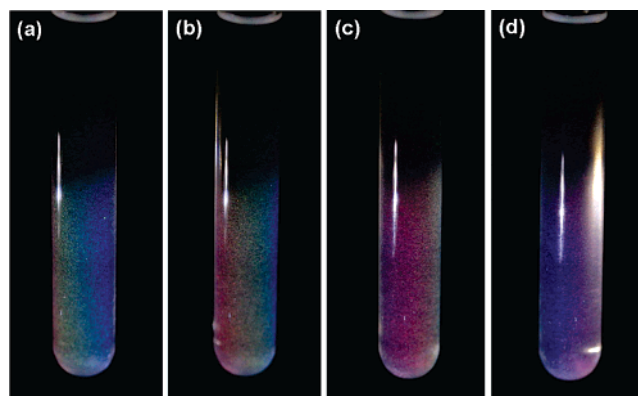


**Figure 10.** Reflective colors of the PS supraballs. At (a) 90 $^{\circ}$ , (b) 60 $^{\circ}$ , (c) 35 $^{\circ}$ , and (d) 10 $^{\circ}$  between the incident beam and the viewing direction. The supraballs were composed of 267 nm PS particles and dispersed in hexadecane.

shifted relative to those of opaline photonic balls. Meanwhile, the band gap of a composite ball composed of the PS microspheres and silica nanoparticles was red-shifted because the reflective index contrast was lowered. These inverse opaline structures have much better photonic band gap properties and are of practical importance for reflective color pigments and chemical and biological sensors.

### Conclusions

We demonstrated self-assembly of colloids inside water-in-oil droplets induced by microwave irradiation. Using the phase-selective microwave heating, we could consolidate the emulsion droplets to photonic balls efficiently within a very short time compared to the conventional methods. The photonic balls that were fabricated at low intensities showed a well-ordered packing quality and optical properties. The reflective colors depended on the size of the constituting particles, the refractive index contrast, and the angle of incident beam relative to the viewing direction. However, the photonic balls displayed an identical reflective color for the normal incident light, because the surface of the photonic balls was the (111) plane of fcc packing. In

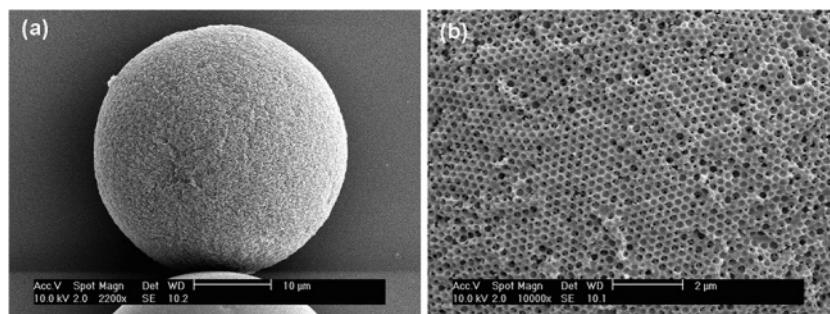


**Figure 11.** (a) SEM images of the inverted supraballs composed of nanometer-sized silica particles of 30 nm in mean diameter and (b) its magnified surface image. The inverse silica supraballs were made by using 267 nm PS particles as sacrificial templates.

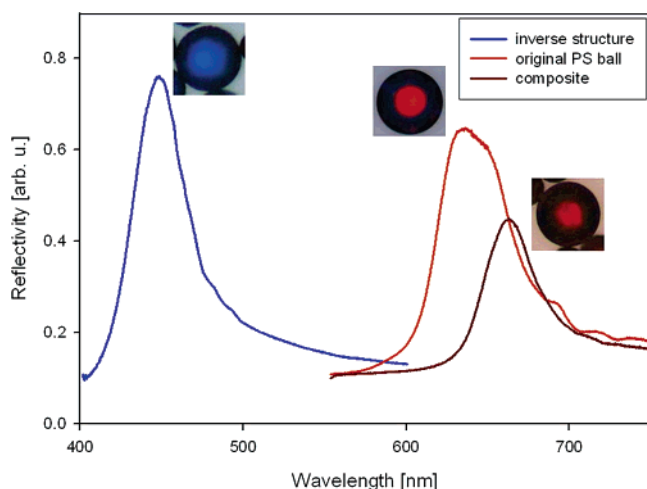


**Figure 12.** Reflectance spectra of the opaline colloidal crystals composed of 267 nm PS particles, their composite and inverse structures.

particular, we could control the packing density of photonic balls composed of polymeric latex particles by changing the intensity of the microwave irradiation, which in turn tuned the photonic band gaps and reflective colors. Our photonic balls can be used

as highly functional pigments, biosensors, and light diffusers. Moreover, if the number of the constituent particles in each droplet is small, we can fabricate colloidal clusters which are useful as colloidal photonic molecules.

**Acknowledgment.** This work was supported by a grant from the Creative Research Initiative Program of the Ministry of Science & Technology for “Complementary Hybridization of Optical and Fluidic Devices for Integrated Optofluidic Systems.” The authors also appreciate partial support from the Brain Korea 21 Program and thank Dr. Hee Young Kim in the Korea Research Institute of Chemical Technology for helpful discussions on microwave-assisted heating.

**Supporting Information Available:** Experimental details are described including materials, experimental procedures, and characterization. Laser scanning confocal microscope images of the internal structures of photonic balls are also included. This material is available free of charge via the Internet at <http://pubs.acs.org>.

JA063528Y